RHIC PERFORMANCE WITH STOCHASTIC COOLING FOR IONS AND HEAD-ON BEAM-BEAM COMPENSATION FOR PROTONS*

W. Fischer†, J. Alessi, Z. Altinbas, E.C. Aschenauer, G. Atoian, E. Beebe, S. Binello, I. Blackler, M. Blaskiewicz, J.M. Brennan, K.A. Brown, D. Bruno, R. Connolly, M. Costanzo, T. D'Ottavio, K.A. Drees, A.V. Fedotov, C.J. Gardner, D.M. Gassner, X. Gu, C. Harper, M. Harvey, J. Hock H. Huang, T. Hayes, R. Hulsart, J. Jamilkowski, T. Kanesue, N.A. Kling, B. van Kuik, J.S. Laster, C. Liu, Y. Luo, D. Maffei, Y. Makdisi, M. Mapes, G.J. Marr, A. Marusic, F. Meot, K. Mernick, R. Michnoff, T.A. Miller, M. Minty, C. Montag, J. Morris, G. Narayan, C. Naylor, S. Nemesure, M. Okamura, S. Perez, A.I. Pikin, P. Pile, A. Poblaguev, V. Ptitsyn, V. Ranjbar, D. Raparia, G. Robert-Demolaize, T. Roser, J. Sandberg, W.B. Schmidke, V. Schoefer, F. Severino, T. Shrey, K. Smith, D. Steski, S. Tepikian, R. Than, P. Thieberger, J. Tuozzolo, G. Wang, K. Yip, A. Zaltsman, A. Zelenski, K. Zeno, W. Zhang, BNL, Upton, New York, USA; M. Bai, Y. Dutheil, FZJ Jülich, Germany; S.M. White, ESRF, Grenoble, France

Abstract

The Relativistic Heavy Ion Collider (RHIC) has two main operating modes with heavy ions and polarized protons respectively. In addition to a continuous increase in the bunch intensity in all modes, two major new systems were completed recently mitigating the main luminosity limit and leading to significant performance improvements. For heavy ion operation stochastic cooling mitigates the effects of intra-beam scattering, and for polarized proton operation head-on beam-beam compensation mitigates the beam-beam effect. We present the performance increases with these upgrades to date, as well as an overview of all operating modes past and planned.

INTRODUCTION

The Relativistic Heavy Ion Collider (RHIC) and the Large Hadron Collider (LHC) are the two heavy ion colliders in the world [1], in heavy ion operation since 2000 and 2010 respectively. RHIC's two main science programs are: (i) the collisions of heavy ions, used to create and characterize the quark gluon plasma (QGP); (ii) the collision of polarized protons, to explore the origin of the proton spin.

To create and characterize the QGP the species combinations (9 to date incl. p+A [2]) and energies (16 to date) of the colliding ions are varied over the widest possible range (Fig. 1). While the LHC reaches a higher collision energy, RHIC spans the transition energy from cold nuclear matter to the QGP, and offers the greatest possible flexibility and longer run times, thus making the two machines complement each other [1]. As a collider of spin-polarized proton beams [3], the injectors and RHIC require a number of special devices including a polarized source [4], snakes and rotators, polarimeters, and stringent controls of orbits and tunes [5]. The luminosity, important in all operating modes, is given [6] by

$$\mathcal{L}(t) = (\beta\gamma)\frac{f_{\rm rev}}{4\pi}k_c\frac{N_B(t)N_Y(t)}{\epsilon_n(t)\beta^*(t)}h(\sigma_s(t),\theta(t)) \quad (1)$$

where $(\beta\gamma)$ are the relativistic factors, $f_{\rm rev}$ is the revolution frequency, k_c is the number of bunch pairs colliding at the IP ($k_c \le k_b$ the total number of bunches), $N_{B,Y}$ the bunch intensities, ϵ_n the normalized rms emittance, and β^* the lattice function at the IP. The factor $h \lesssim 1$ captures the geometric luminosity reduction due to the hourglass effect with bunch length σ_s, and a crossing angle θ. With equal ion species we have $\mathcal{L} \propto N_B N_Y = N_b^2$, and typically the largest gains in $\mathcal{L}$ can be made by increasing N_b.

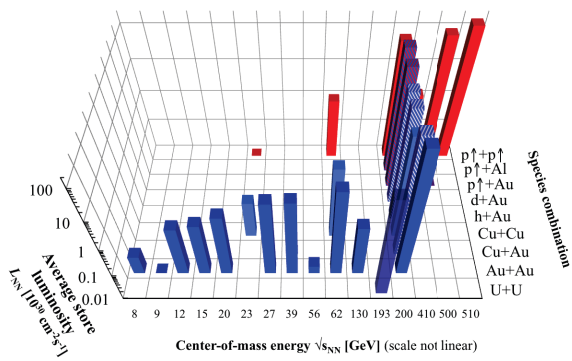

Figure 1: Center-of-mass energy $\sqrt{s_{NN}}$ and nucleon-pair average store luminosity L_{NN} for all species combinations in RHIC to date [7].

To compare different species the nucleon-pair luminosity $\mathcal{L}_{\rm NN} = A_1 A_2 \mathcal{L}$ is used (mass numbers $A_{1,2}$), and the time-integrated luminosity is $L_{\rm NN} = \int \mathcal{L}_{\rm NN}(t)dt$. With beam polarizations $P_{B,Y}$ for the Blue and Yellow beams the figure of merit (FOM) in polarized proton operation is $LP_{B,Y}^2$ ($LP_B^2P_Y^2$) for single (double) spin experiments.

The RHIC science program is mapped out until 2023, after which it is planned to construct the electron-ion collider

* Work supported by Brookhaven Science Associates, LLC under Contract No. DE-AC02-98CH10886 with the U.S. Department of Energy.
† Wolfram.Fischer@bnl.gov

ISBN 978-3-95450-147-2

eRHIC [8]. 2019 and 2020 will be dedicated to the operation below and up to the nominal injection energy, in search of a critical point in the nuclear matter phase diagram. At these energies the luminosity is low (Fig. 1) because of the large beam size, magnetic field errors, intrabeam scattering, and space charge [9]. For a 4-fold increase in the luminosity, a bunched beam electron cooler is under construction for the lowest energies [10].

HEAVY ION OPERATION WITH STOCHASTIC COOLING

Luminosity limits in Au+Au operation. The primary limits to the Au+Au luminosity in RHIC [1] are the bunch intensity available from the injectors, a fast transverse transition instability in RHIC, intrabeam scattering in RHIC, machine and experimental protection issues, and presently the RF amplifier power for the Landau cavities in RHIC.

The bunch intensity N_b has been steadily increased (Fig. 2) by: a γ_t-jump and octupoles at transition (2002), scrubbing with protons, and an increasing number of bunch merges in the Booster and AGS [11]. With the merges the longitudinal emittance must fit into the limited acceptance of the RHIC 197 MHz storage RF system. Fast transverse instabilities at transition [12] have limited the intensity in the past, but after vacuum upgrades and due to scrubbing in proton operation [13] this is presently not a limit. A new EBIS pre-injector is used since 2012 [14], with input from a laser ion source since 2014 [15].

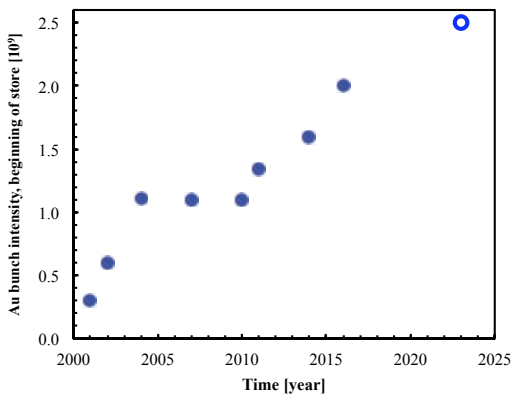

Figure 2: Au bunch intensity evolution in RHIC. The ultimate intensity goal is given for 2023.

Stochastic cooling in RHIC. While stochastic cooling was and is used in a number of low-energy storage rings, RHIC is the first collider with operational stochastic cooling. Cooling in a longitudinal plane was demonstrated in 2006 using a low intensity proton bunch with 10^9 particles. Operational longitudinal cooling of gold ions in one of the rings was demonstrated the following year, and full 3D cooling is available in both rings since 2012.

Ion beams are composed of bunches of full width 5 ns separated by 107 ns. Cooling times of about 1 h are obtained with a 3 GHz system bandwidth and optimal kicker voltages of typically 3 kV. A wideband kicker would require very high microwave power. To reduce the power a set of kicker cavities with only 10 MHz bandwidth was adopted that takes advantage of the bunch spacing. An overview of the system is shown in Fig. 3, and a detailed description is given in Ref. [16].

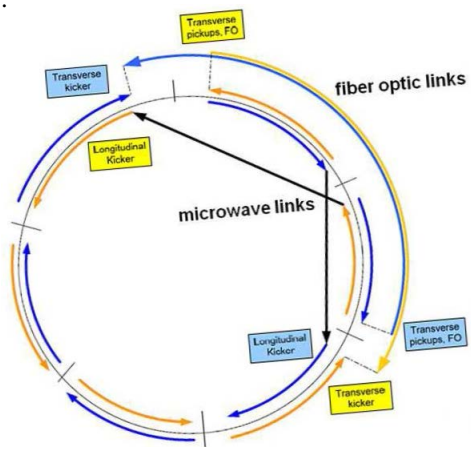

Figure 3: Overview of the RHIC stochastic cooling system. Each plane (horizontal, vertical, longitudinal) has a pick-up and a set of kickers. Information travels from the pick-up to the kickers via fiber-optic links for the transverse planes, and via a microwave link in the longitudinal planes.

Operation with stochastic cooling. Figure 4 shows the dramatic effect the increase in N_b had on the initial luminosity, and stochastic cooling on the luminosity lifetime with the increased intensity. The 2014 luminosity starts at a much higher value but still decays for about half an hour before the cooling takes full effect. The cooling then reduces the beam sizes fast enough that the luminosity begins to increase, and typically exceeds the initial value. It then decays over time, as more and more ions are lost in the collision process. The 2014 stores end with luminosity values as high as the initial values in 2007 [17].

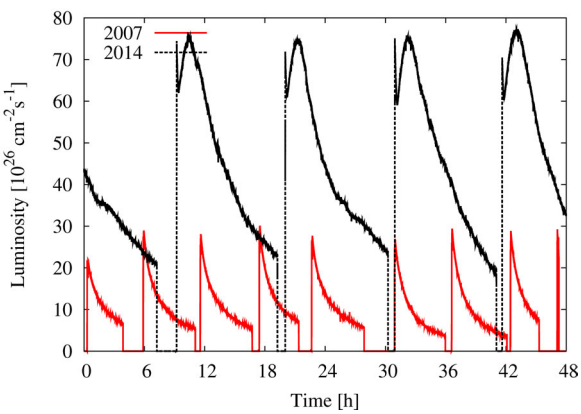

Figure 4: Luminosity delivered to the PHENIX over 48 h in 2007 with longitudinal stochastic cooling in the Yellow Ring only, and in 2014 with 3D cooling in both rings.

With stochastic cooling RHIC operates close to the burn-off limit, i.e. the dominant particle loss is from the collisions [18]. With cooling it is also possible to tolerate tran-

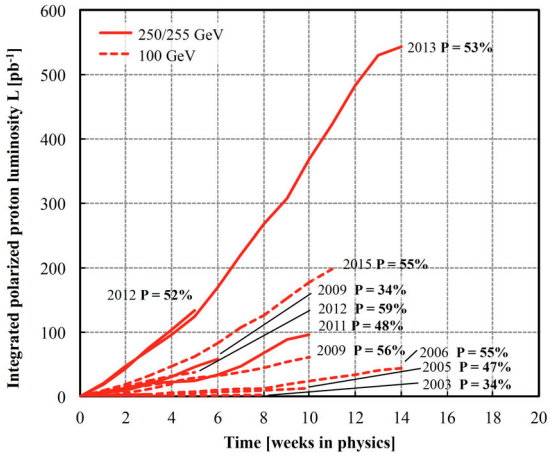

Figure 5: Intensities (top, left scale), beam loss rates measured and calculated for burn-off (top, right scale), rms emittances of all four planes (center), and luminosities (bottom) in Au+Au operation in 2016.

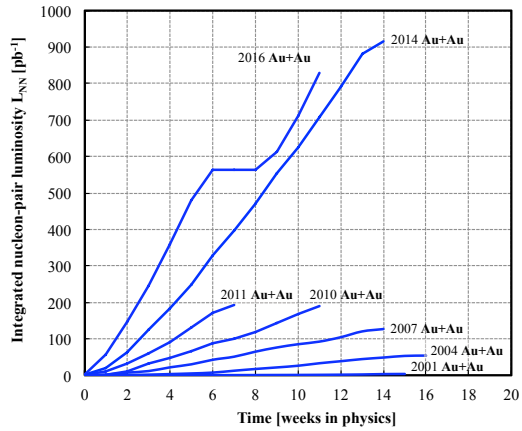

Figure 6: Integrated nucleon-pair luminosity L_{NN} for all Au+Au runs. The 2-week plateau in 2016 is due to the replacement of a shorted quench protection diode. The 2016 run was still ongoing at paper submission.

Table 1: Main Design, Achieved and Upgrade Parameters for Au Beams in RHIC [7]

parameter	unit	design 2000†	achieved 2016	upgrade ≥2022
circumference C	km	— 3.834 —		
beam energy E	GeV/n		— 100 —	
bunch intensity N_b	10^9	1.0	2.0	2.5
no of bunches k_b	...	60	111	111
stored beam energy	MJ/beam	0.12	0.70	0.88
rms emittance ϵ_n	μm		— 2.5 —	
rms bunch length σ_s	m		— 0.3 —	
beam-beam ξ/IP	10^{-3}	2.3	3.1	3.8
lattice β^*	m	2.0	0.7	0.6
luminosity $\mathcal{L}_{peak}$	10^{26}cm^{-2}s^{-1}	8	130	200
luminosity $\mathcal{L}_{avg}$	10^{26}cm^{-2}s^{-1}	2	83	160

† Column gives the design values. 2000 is the first year of operation.

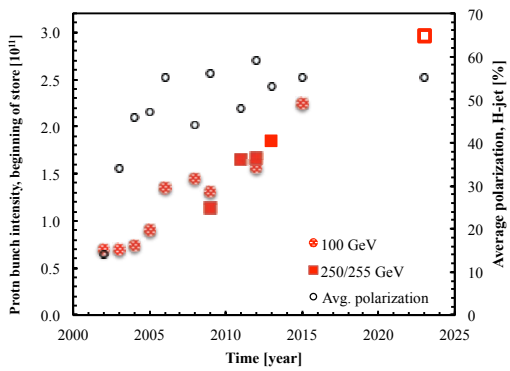

Figure 7: Polarized proton bunch intensity evolution (left scale), and average beam polarization. The ultimate goals are given for 255 GeV in 2023.

sition instabilities as long as they do not lead to intensity losses, and the emittance growth does not lead to excessive losses with the standard collimator settings at store.

During the 2016 operation one of the two experiments had a maximum luminosity limit of 60×10^{26}cm^{-2}s^{-1} (Fig. 5). With this requirement the cooling strength at the beginning of the store is reduced but large enough to have beam loss rates close to the burn-off rate. With the almost flat luminosities of both experiments in the later part of the store, N_b decreases linearly with time.

The overall RHIC performance in Au+Au operation is summarized in Table 1 and Fig. 6. The integrated luminosity of the run at 100 GeV/nucleon in 2014 exceeds the combined integrated luminosities of all previous Au+Au runs. With further increases in the bunch intensity, and upgrades to the RHIC RF systems it is planned to increase the average store intensity by another factor of two (Table 1).

PROTON OPERATION WITH HEAD-ON BEAM-BEAM COMPENSATION

Luminosity limits in polarized p+p operation. The luminosity in polarized proton operation in RHIC is primarily limited by two effects [1]. First, the need to maintain high polarization in the RHIC bunches limits the available intensity [3], and second, the beam-beam effects limit the brightness N_b/ϵ_n [19].

The polarized proton bunch intensity has been steadily increased, without a reduction in the polarization (Fig. 7), by: adding the AGS warm snake (2004) [20], upgrading the source superconducting solenoid (2005), adding the AGS cold snake (2006) [21], the AGS tune jump system [22] and RHIC 9 MHz RF system (2011), the polarized source upgrade with Atomic Beam Source (2013) [4]. The higher intensity also required a RHIC abort kickers upgrade [23].

Head-on beam-beam compensation in RHIC. The compensation scheme in RHIC requires a new lattice and electron lenses. The transverse kick $\Delta r'_{pp}$ a particle receives

ISBN 978-3-95450-147-2

when passing through the other beam is reversed in the same turn when the particle passes through an electron lens and receives the kick $\Delta r'_{pe}$. For exact compensation at all amplitudes r one needs: (i) Electron lens at a phase advance of $k\pi$, k integer, after the beam-beam interaction to minimize the resonance driving terms; (ii) Amplitude dependence of the correction kick $\Delta r'_{pe}(r)$ equal to the beam-beam interaction, $\Delta r'_{pp}(r)$ to reduce the tune spread [24].

Electron lenses were first used in the Tevatron where they operated as abort gap cleaner and demonstrated a better lifetime of bunches with long-range beam-beam effects. Hollow electron lenses were tested as collimation devices [25]. The RHIC lenses are described in [24, 26].

Instrumentation is a critical part of the electron lens operation as the electron and proton beams need to overlap with a deviation of only a fraction of an rms beam size. This is reliably achieved with a novel monitor that detects electrons backscattered by the protons [27], and allows for a fast and robust alignment of the beams.

The electron lens compresses the beam-beam induced tune spread. This is shown in Fig. 8, where the incoherent tune spread is obtained from a transverse beam transfer function (BTF) as the non-zero imaginary part of the complex BTF $R(Q)$, i.e. $\mathrm{Im}(R) > 0$ [28]. The measurement is with p+Al collisions since, different from p+p operation, the fractional tunes in the two beams differ by a value much larger than the beam-beam parameter ξ_p, and therefore the beams exhibit no coherent oscillation modes when excited.

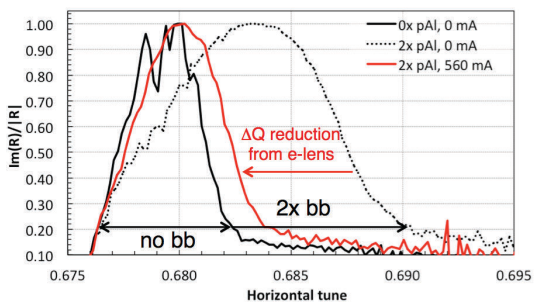

Figure 8: Tune distribution width reduction with the electron lens, measured in the proton beam with p+Al collisions. The distribution widens due to two beam-beam interactions, and narrows again with the electron lens [24].

Operation with head-on beam-beam compensation. For operational use [29] it was verified that the electron lenses do not introduce additional emittance growth, and only small additional beam losses (1-2%/h). The increased loss rate did not measurably affect the luminosity as it stems from particles in the tails that contribute little to the luminosity. For physics stores the electron lenses were turned on while the electron and proton beams were transversely separated (Fig. 9, no 1) and before the proton beams went into collision. Then collisions were established in one experiment (Fig. 9, no 2), which allowed to set the collimators to store positions. In a third step (Fig. 9, no 3) the beams went into collision

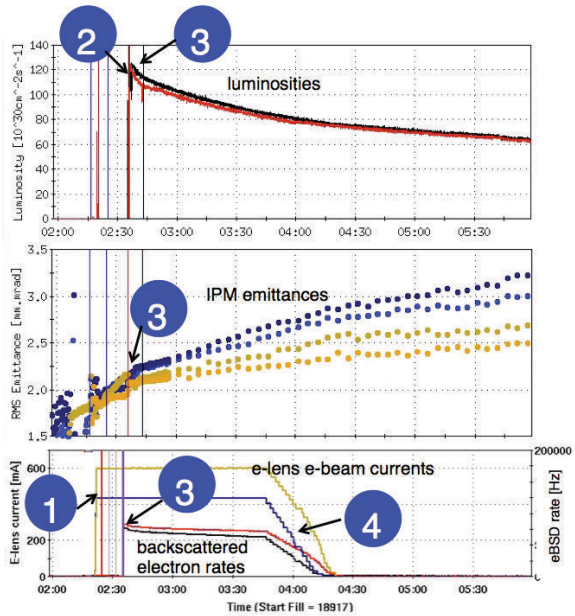

Figure 9: Luminosities, emittances, electron lens currents, and rates of the backscattered electron detectors in polarized p+p operation in 2015. The sequence of events marked by the numbers is explained in the text.

in the second experiment and the electron lenses simultaneously. Due to the tune compression, higher beam-beam parameters can be accommodated with the lenses. With too large beam-beam parameters $|\xi_p|$ fast emittance growth or larger beam loss rates can be observed. After commissioning, 112 out of 156 p+p stores used both electron lenses, without any turn-on failure. After approximately 1 h the lattice alone could support the beam-beam parameters with the highest available brightness available from the injectors in 2015, and the lenses were gradually ramped down (Fig. 9, no 4).

Table 2 summarizes the increases in bunch intensity, beam-beam parameter and luminosity from 2012 to 2015. The new lattice alone could support a higher beam-beam parameter. Since the electron lenses never failed to turn on there are no operational data for the maximum beam-beam parameter without the electron lens. These were determined in dedicated tests. Figure 10 shows the initial emittance and its increase over 5 min after going into collision (top), and the intensity reduction over 5 min (bottom) for all operational stores and the test for maximum $|\xi_p|$. The dotted horizontal lines show the average of good operational stores and are used as benchmark to define acceptable beam-beam parameters. The dashed vertical lines show the maximum beam-beam parameters reached without and with the electron lenses (also in Table 2). Simulations for 2015 are in Ref. [31].

The overall RHIC performance in polarized proton operation in summarized in Table 3 and Fig. 11. The integrated luminosities of the recent runs at 255 GeV in 2013 and 100 GeV in 2015 both exceed the combined integrated lumi-

Table 2: Main Parameters for Polarized p+p Operation at 100 GeV in 2012 (Without) and 2015 (With Head-On Beam-Beam Compensation), and conditions for the maximum beam-beam parameters achieved in operation and tests in 2015 without and with electron lenses [24]

quantity	unit	operations avg. over 10 best stores		tests for max $\lvert\xi_p\rvert$		
				without e-lens	with e-lens	with e-lens
		2012	2015	— 2015 —		
bunch intensity N_b	10^{11}	1.6	2.25	2.6	2.15	2.0
no of bunche k_b	...	109	111	48	111	30
rms emittance ϵ_n	μm	3.3	2.8	3.5	2.4	1.9
beam-beam ξ_p/IP	0.001	−5.8	−9.7	−9.1	−10.9	−12.6
# of beam-beam IPs	...	2	2+1*	2	2+1*	2+1*
lumi. $\mathcal{L}_{peak}$	10^{30}cm^{-2}s^{-1}	46	115	72	115	40

*One p+p collision in IP6 and IP8, and a compensating p+e collision in IR10.

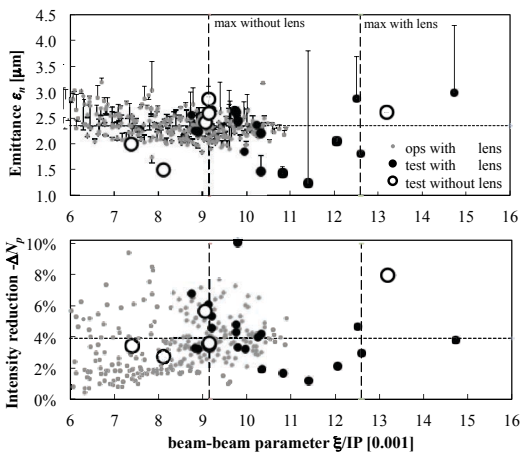

Figure 10: Top: initial emittance and increase after 5 min (vertical lines) as a function of the beam-beam parameter. Bottom: reduction in the bunch intensity over 5 min [24].

nosities of all previous runs at these energies. With the demonstration of head-on beam-beam compensation in the 2015 run it is planned to increase the average store luminosity further by a factor 3 – 4 (Table 3). For this an increase in the polarized bunch intensity is necessary, which can be accomplished with a higher source output [4] and better transmission in the AGS.

SUMMARY

The implementation of stochastic cooling, the first operating cooling system in a collider, together with an increase in the bunch intensity led to a 7-fold increase in the average store luminosity to date. The increased bunch intensity N_b primarily accounts for the higher initial luminosity $\mathcal{L}_{init}$, while the stochastic cooling system reduces the beam loss rates close to the burn-off rates. The average store luminosity now exceeds the design value by a factor of 40, and another increase by a factor 2 is planned.

A head-on beam-beam compensation scheme, consisting of a new lattice and electron lenses, was used for the first

Table 3: Main Design, Achieved and Upgrade Parameters for Polarized Proton Beams in RHIC [7]

parameter	unit	design 2004	achieved 2015/13	upgraded ≥2022
beam energy E	GeV	100/250	100/255	100/255
bunch intensity N_b	10^{11}	2.0/2.0	2.25/1.85	3.0/3.0
no of bunches k_b	...		— 111 —	
stored beam energy	MJ/beam	0.36/0.87	0.40/0.84	0.53/1.34
rms emittance ϵ_n	μm	2.5	2.8/3.1	2.5/2.5
rms bunch length σ_s	m	0.87/0.55	0.70/0.60	0.50/0.50
beam-beam ξ/IP	10^{-3}	9.6	9.7/7.2	15/15
lattice β^*	m	1.0/1.0	0.85/0.65	0.85/0.50
luminosity $\mathcal{L}_{peak}$	10^{30}cm^{-2}s^{-1}	90/250	115/245	270/1000
luminosity $\mathcal{L}_{avg}$	10^{30}cm^{-2}s^{-1}	60/150	63/160	175/600
polarization P_{avg}	%	70	57/52	60/55

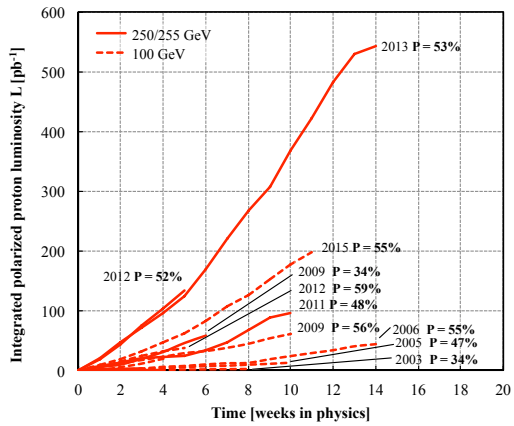

Figure 11: Integrated luminosity for all polarized p+p runs.

time in 2015 with polarized protons at 100 GeV, and approximately doubled the luminosity compared to the last run in 2012 at the same energy by allowing for an increase in N_b. With demonstrated tune footprint compression, and reliable operation of the lenses, the luminosity is presently limited by the intensity and brightness available from the injectors while maintaining high polarization, and a further luminosity increase by a factor 3-4 is planned.

ACKNOWLEDGEMENTS

The authors wish to thank the members of the Collider-Accelerator Department at Brookhaven National Laboratory who have supported the operation and upgrades of RHIC and its injectors, and collaborators from other laboratories, in particular Fermilab and CERN.

REFERENCES

[1] W. Fischer and J. Jowett, RAST 07, pp. 49-76 (2014).

[2] C. Liu *et al.*, presented at IPAC'16, Busan, Korea, May 2016, paper TUPMW038, this conference.

[3] M. Bai *et al.*, IPAC13, pp. 1106-1110 (2013).

[4] A. Zelenski *et al.*, IOP JoP, Conf. Series 295, 012147 (2011).

[5] M. Minty *et al.*, PAC11, pp. 1394-1396 (2011).

ISBN 978-3-95450-147-2

[6] M. Furman, Luminosity, in A.W. Chao *et al. Handbook of accelerator physics and engineering*, 2nd ed. (World Scientific, 2013), pp. 311-318.

[7] www.rhichome.bnl.gov/RHIC/Runs

[8] V. Ptitsyn *et al.*, presentation at ERL2016; A. Aschenauer *et al.*, BNL-108524-2015-IR, eRHIC/46 (2015).

[9] T. Satogata *et al.*, PoS(CPOD 2009)052 (2009).

[10] A. Fedotov, ICFA BD Newsletter No. 65, p. 22 (2014).

[11] C.J. Gardner *et al.*, IPAC15, pp. 3804-3806 (2015).

[12] M. Blaskiewicz, PAC03, pp. 3026-3028 (2003).

[13] W. Fischer *et al.*, PRSTAB 11, 041002 (2008).

[14] J. Alessi *et al.*, PAC11, pp. 1966-1968 (2011).

[15] T. Kanesue *et al.*, IPAC14, pp. 1890-1892 (2014).

[16] M. Blaskiewicz and J.M. Brennan, PRSTAB 10, 061001 (2007); J.M. Brennan, M. Blaskiewicz, and F. Severino, PRL 100, 174802 (2008); M. Blaskiewicz, J. M. Brennan, and K. Mernick, PRL 105, 094801 (2010).

[17] G. Robert-Demolaize *et al.* IPAC14, pp. 1090-1092 (2013).

[18] W. Fischer *et al.*, PRC 89, 014906; presented at IPAC'16, Busan, Korea, May 2016, paper TUPMW039, this conference. TUPMW039.

[19] Y. Luo, W. Fischer, and S. White, PRAB 19, 021001 (2015).

[20] M. Okamura *et al.*, EPAC02, pp. 2421-2423 (2002); H. Huang *et al.*, PRL 99, 154801 (2007)

[21] R. Gupta *et al.*, PAC03, 1936-1938 (2003).

[22] V. Schoefer *et al.*, IPAC12, pp. 1015-1019 (2012).

[23] C. Montag *et al.*, presented at IPAC'16, Busan, Korea, May 2016, paper TUPMW043, this conference.

[24] W. Fischer *et al.*, PRL 115, 264801 (2015).

[25] V. Shiltsev *et al.*, PRSTAB 11, 103501 (2008); X.-L. Zhang *et al.*, PRL 99, 244801 (2007); G. Stancari *et al.*, PRL 107, 084802 (2011); V. Shiltsev, "Electron lenses for super colliders", Springer (2016).

[26] X. Gu, M. *et al.*, NIMA 637, pp. 190-199 (2011); X. Gu *et al.*, NIMA 743, pp. 56-67 (2014); X. Gu *et al.*, NIMA 798, pp. 36-43 (2015).

[27] P. Thieberger *et al.*, PRAB 19, 041002 (2016).

[28] A.W. Chao, "Physics of collective beam instabilities in high energy accelerators", John Wiley & Sons, Chapter 5 (1993).

[29] V. Schoefer *et al.*, IPAC15, pp. 3612-3614 (2015).

[30] Y. Luo *et al.*, presented at IPAC'16, Busan, Korea, May 2016, paper TUPMW040, this conference.

ISBN 978-3-95450-147-2